

Research Article

Effect of Physical and Chemical Activation on the Removal of Hexavalent Chromium Ions Using Palm Tree Branches

Soheir Khedr, Mona Shouman, Nady Fathy, and Amina Attia

Surface Chemistry and Catalysis Laboratory, National Research Center, El-Dokki, Cairo 12622, Egypt

Correspondence should be addressed to Amina Attia; amina_abdelmeguid@yahoo.com

Received 23 February 2014; Accepted 13 March 2014; Published 2 April 2014

Academic Editors: D. Petruzzelli and C. Waterlot

Copyright © 2014 Soheir Khedr et al. This is an open access article distributed under the Creative Commons Attribution License, which permits unrestricted use, distribution, and reproduction in any medium, provided the original work is properly cited.

Nowadays the removal of heavy metals from wastewater is essential due to their high toxicity and impact on human health. In the present study, branches of palm trees were converted into activated carbon by chemical and physical activation. The prepared samples were used for the removal of Cr(VI) from their aqueous solution. Chemical activation was carried out using (20 and 50%) H_3PO_4 and K_2CO_3 , and physical activation was performed using steam. Batch adsorption experiments were carried out to examine the removal process under factors such as pH and pH_{pzc} . The metal ion removal was pH dependent and reached maximum removal at pH 2. Experimental data were analyzed using Langmuir, Freundlich, and Flory-Huggins isotherms. The adsorption studies revealed that the removal of Cr(VI) ions was well fitted with Langmuir isotherm. The adsorption kinetics well fitted using a pseudo second-order kinetic model. Column studies revealed that the highest bed volume (60 BV) was observed for the sample activated with 50% H_3PO_4 . The adsorption efficiency was enhanced with acid treatment (50% H_3PO_4) and reduced by steam.

1. Introduction

The discharge of heavy metals into the environment has been increasing continuously due to rapid industrialization and has created a major global concern. The release of these heavy metals causes a significant hazard to human health and the environment because of their toxicity, accumulation in living tissues, and consequent biomagnifications in the food chain [1, 2].

Among the different heavy metals in concern is chromium. Compounds of chromium mainly occur in the environment as trivalent Cr(III) and hexavalent Cr(VI). Trivalent chromium is an essential element in human nutrition (especially in glucose metabolism) and is less toxic than the hexavalent state, which is recognized as a carcinogenic and mutagenic agent [3]. Acute exposure to high levels of Cr(VI) can produce nervous system damage and liver disorder. EPA (Environmental Protection Agency) has set the maximum level of total Cr concentration allowed in drinking water at 0.1 mg L^{-1} [4]. Chromium and its compounds are widely used in electroplating, leather tanning, cement, dyeing, metal processing, wood preservatives, paint and pigments, textile, steel fabrication,

and canning industries. In Egypt, about 2000–5000 tons of chromium pollute the environment annually from several industries in the aqueous effluent compared to the recommended permissible discharge limits of 2 mg L^{-1} [5].

Conventional methods for removing dissolved heavy metal ions include chemical precipitation, chemical oxidation or reduction, filtration, ion exchange, electrochemical treatment, and membrane technology [6]. However, these processes have significant disadvantages such as incomplete metal removal, high reagent and energy requirements, and generation of toxic sludge or other waste products that require disposal [7].

Adsorption is an economical alternative to conventional metal removal techniques [8]. The most widely used industrial adsorbent is activated carbon. Activated carbon adsorption has proved to be the least expensive treatment option, particularly in treating low concentrations of wastewater streams. Activated carbons are carbonaceous materials that have highly developed porosity, internal surface area, and relatively high mechanical strength [9, 10]. In recent years, investigations have been carried out for the effective removal of large quantities of Cr(VI) from wastewater using low-cost, nonconventional adsorbent [11, 12].

Egypt is one of the largest countries which produce Palm trees. Palm trees represent 6.32% of the fruit cultivated area in Egypt. They are mainly located in the Nile Delta, Nile Valley, and South and North Sinai [13]. Palm tree branches have the characteristic of exchange sorption properties due to the presence of some functional groups such as carboxylic, hydroxyl, and lactone which have a high affinity for metal ions.

In the present investigation, different types of activated carbon were prepared using Palm tree branches for the removal of Cr(VI) from prepared aqueous solutions. The methods used for activation of Palm tree branches can be carried out in two different methods, which are physical and chemical activation. In physical activation, the precursor is first carbonized in an inert atmosphere (N_2 gas) and then activated in a stream of steam, whereas for chemical activation, the precursor was impregnated with (20 and 50%) H_3PO_4 and K_2CO_3 . Chemical activation was characterized by low energy cost and also has better development of porous structure [14]. The main objective of this research is to evaluate the efficiency of carbon adsorbents prepared from Palm tree branches for the removal of Cr(VI) ion from aqueous solutions. The effect of pH and pH_{pzc} was investigated. Adsorption, kinetics, column, and desorption studies were also conducted.

2. Materials and Methods

2.1. Sample Collection and Treatment. The Palm tree branches were collected from the institute campus. The biomass was extensively washed with distilled water to remove dust and soluble impurities. The branches were then cut into small pieces and kept dried in an oven at $80^\circ C$ for overnight. The dried biomass was ground in a laboratory blender and sieved to desired mesh size of 2-3 mm.

2.2. Preparation of Adsorbent Materials. For chemical activation, the samples were prepared by mixing 40 gm of Palm tree branches with 100 mL of 20% and 50% H_3PO_4 (m/v), respectively. The phosphoric acid soaked samples are left overnight in ambient environment and the excess water was evaporated in oven $100^\circ C$ to ensure complete absorbance of the phosphoric acid onto the Palm tree branch. The acid soaked samples were dried in a hot air oven at $110^\circ C$ for 1 h. Then, the materials were activated in a muffle furnace at $500^\circ C$ for 2 h. The activated carbon samples were washed with distilled water, respectively, until $pH \sim 7$ was attained to remove any acid content. The samples were then dried in an oven at $110^\circ C$ to remove any moisture content. The samples obtained were labeled as APBH20 and APBH50. As for the second activating agent, 50 g of K_2CO_3 was added to 50 g of Palm tree branch (w/w). Afterwise, 100 mL of distilled water was added to the beaker and then dehydrated in an oven at $110^\circ C$ followed by heating in a muffle furnace at $800^\circ C$ for 1 h. The sample obtained was labeled as APBK.

For physical activation, the Palm tree branches were prepared by introducing 40 g of the dried ground material into a quartz vertical tube fitted with an internal perforated

TABLE 1: Characteristics of different adsorbents investigated.

Parameter	Adsorbents				
	RPB	APBH 20	APBH 50	APBS	APBK
S_{BET} ($m^2 g^{-1}$)	147	157	401.3	90	215
Pore volume ($cm^3 g^{-1}$)	0.014	0.070	0.134	0.029	0.091
Pore radius (\AA)	7.4	7.2	7.3	7.1	7.2
pH_{pzc}	4.1	4.3	3.7	6.7	7.5

quartz diaphragm. Steam was generated in a round-bottom flask placed in a heating mantle and directly admitted at the top of the carbonization tube. The pyrolysis reactor was surrounded by a temperature controlled electrical furnace. The gas steam product exited to a water-cooled condenser, and the noncondensable gases were vented through a gas hood (fume cupboard). Heating was conducted at about 10°min^{-1} until $350^\circ C$, and then steam was introduced and heating continued at a slower rate 5°min^{-1} until the required temperature $700^\circ C$ was attained for 1 h. After cooling, the product was weighed to estimate the yield. The sample obtained was labeled as APBS.

2.3. Characterization of the Adsorbents. The textural characteristics of the different biosorbents studied were determined by N_2 adsorption isotherm at 77 K isotherm using BET analyzer (Quantachrome AS1 Win, Version 2.01, USA). FTIR analysis was conducted using a Perkin Elmer Spectrum RX FTIR within a range of $400\text{--}4000 \text{ cm}^{-1}$. The morphology of the biosorbents was analyzed by scanning electron microscope using JEOL 56OLV SEM at 20 KeV with background subtraction and a summation of 60 scans. The physical parameters of the different activated carbons studied are shown in Table 1.

2.4. Batch Adsorption Experiments. A stock solution of Cr(VI) was prepared by dissolving 2.8 g of potassium dichromate (99.9% $K_2Cr_2O_7$) in 1 L distilled water. This solution is diluted as required to obtain solutions containing different concentrations ($20\text{--}100 \text{ mg L}^{-1}$) of Cr(VI). 1 M HCl and 1 M NaOH solutions were prepared for pH adjustment. The batch experiments were carried out in 100 mL conical flasks by agitating a preweighed amount of the Palm-activated carbon adsorbents with 50 mL of the aqueous Cr(VI) solutions. The test solutions were agitated on a rotary shaker at 250 rpm min^{-1} . A purple-, violet-colored complex was developed in the reaction between Cr(VI) and 1, 5 diphenyl-carbazide in acidic condition. The absorbance of the purple violet color for Cr(VI) was determined spectrophotometrically (Shimadzu UV-Vis I204PC) at 540 nm after 20 min [15].

The pH measurements were done with a pH electrode (Systronics); however, the pH_{pzc} was determined by pH drift method [16]. This method was conducted to determine the pH_{pzc} of Palm tree activated carbons. The pH_{pzc} is the point in which the pH (initial) = pH (final).

The amount of Cr adsorbed by the different activated carbons studied was calculated using the following equation:

$$q_e = \frac{(C_o - C_e)V}{W}, \quad (1)$$

where q_e is the amount of Cr(VI) adsorbed by the adsorbent (mg g^{-1}), C_o and C_e are the initial and equilibrium concentration of Cr(VI), respectively, (mg L^{-1}), V is the initial volume of Cr solution (mL), and W is the weight of the adsorbent (g).

2.5. Column Adsorption Studies. Continuous flow adsorption studies were conducted in a glass column of inner diameter 2 cm, 30 cm height, and 60 mm bed height. The adsorbents containing Cr(VI) solution with initial concentration 100 mg L^{-1} was pumped into the column with constant flow rate 2 mL min^{-1} . The pH of the solution was kept constant throughout the experiments ($\text{pH} = 2$) using 1 M NaOH or 1 M HCl. The effluent solution was collected at regular time intervals, and the equilibrium concentration was measured using UV-vis spectrophotometer.

2.6. Desorption Studies. In order to determine the reusability of the adsorbents, adsorption-desorption cycles were repeated consecutively three times. The regeneration study was performed using a glass column with inner diameter 20 mm and 300 mm length. The column was packed with 1 g of each of the different adsorbents and loaded with 100 mg L^{-1} Cr(VI) solution at a constant speed of 2 mL min^{-1} . Desorption of Cr(VI) ions was performed by using 0.1 M HCl solution. The final Cr(VI) concentration in the aqueous phase was determined by using a spectrophotometer. After each cycle of adsorption-desorption, distilled water was passed through the column to remove any traces of undesorbed Cr(VI).

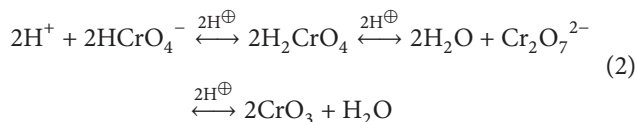
3. Results and Discussion

3.1. Scanning Electron Microscopy Studies. Scanning electron microscopy was used to study the surface morphology and pore size of the untreated and treated modified Palm tree branches (Figures 1(a)–1(e)). Comparing all the figures, Figure 1(c) has the highest development of pores which was attributed to the increase in H_3PO_4 concentration. This led to the creation of new pores and widening of the existing pores [8]. However, as shown in Figure 1(d) the white particles that appear for the Palm tree branches activated with K_2CO_3 may be due to the residue of the activating agent which was not completely reacted during the activation process. Figure 1(e) for steam activation shows that some components might have interfered with the surface of the treated sample and thus lead to shrinkage of the wider pores.

3.2. Fourier Transform Infrared Spectroscopy (FTIR) Analysis. The FTIR spectra provide valuable information about the chemical compositions of the materials. Figure 2 shows the FTIR spectra of the raw and the different activated carbons. Although the samples were prepared via various activation

methods, there was a similarity in the FTIR patterns. Basically all the samples showed a very weak broad peak around $3412\text{--}3452 \text{ cm}^{-1}$ which indicates the presence of hydroxide group in the samples. A slight shift in the pattern was due to the effect of modification process on the surface of the adsorbents. It was suggested that the samples trap moisture on their surface during sample handling due to their adsorptive nature [17]. The peak at 2934 cm^{-1} was found only in the raw sample, which corresponds to the C–H sp^3 stretching. A strong conjugated C=C peak was also observed around $1623\text{--}1633 \text{ cm}^{-1}$ for the raw and sample treated with K_2CO_3 . All samples show a peak around 1446 cm^{-1} which represent C–H deformation. The peaks at 1174 cm^{-1} and 1090 cm^{-1} represent C–O stretching in alcohols and phenols. The shoulder and the bands at lower wave numbers ranging from 600 to 400 cm^{-1} might be related to out-of-plane bending models [17]. The presence of these functional groups may be responsible for good adsorptive behavior of the different modified samples towards Cr(VI) removal.

3.3. Effect of pH. The pH of the solution is one of the prime factors that drastically influence the adsorption behavior, which affects surface charge of the adsorbent material, degree of ionization and specification of adsorbate [18]. In the present study, the effect of pH was examined by varying the solution pH from 2 to 12 using initial metal ion concentration of 100 mg L^{-1} at room temperature. Figure 3 displays the variation of solution pH on the percentage removal of the metal ions from the solution for the different adsorbents studied. Cr(VI) may exist in the aqueous phase in different anionic forms such as chromate (CrO_4^{2-}), dichromate ($\text{Cr}_2\text{O}_7^{2-}$), or hydrogen chromate (HCrO_4^-). The following reaction mechanism for adsorption of Cr(VI) at different pH is proposed by Bayat [19]:



It is well known that the dominant form of Cr(VI) at lower pH is HCrO_4^- [20]; therefore, the electrostatic attraction occurred between the positively charged of the adsorbent and negatively charged HCrO_4^- . However, increasing the pH will shift the concentration of HCrO_4^- to other forms (CrO_4^{2-} and $\text{Cr}_2\text{O}_7^{2-}$). The decrease in Cr(VI) ions removal might be due to the competition between OH^- ion and chromate (CrO_4^{2-}), where the former being the dominant species wins the race. Inspection of Figure 3 revealed that Cr(VI) was found to exhibit different pH dependence with the highest percentage removal occurring at $\text{pH} = 2$.

3.4. The pH_{pzc} of the Adsorbents. The pH_{pzc} is defined as the pH of the suspension at which the surface acidic (or basic) functional groups of adsorbents no longer contribute to the pH value of the solution [21]. The relationship between pH_{pzc} and adsorption capacity is that cations adsorption on any adsorbent will be expected to increase at pH value higher

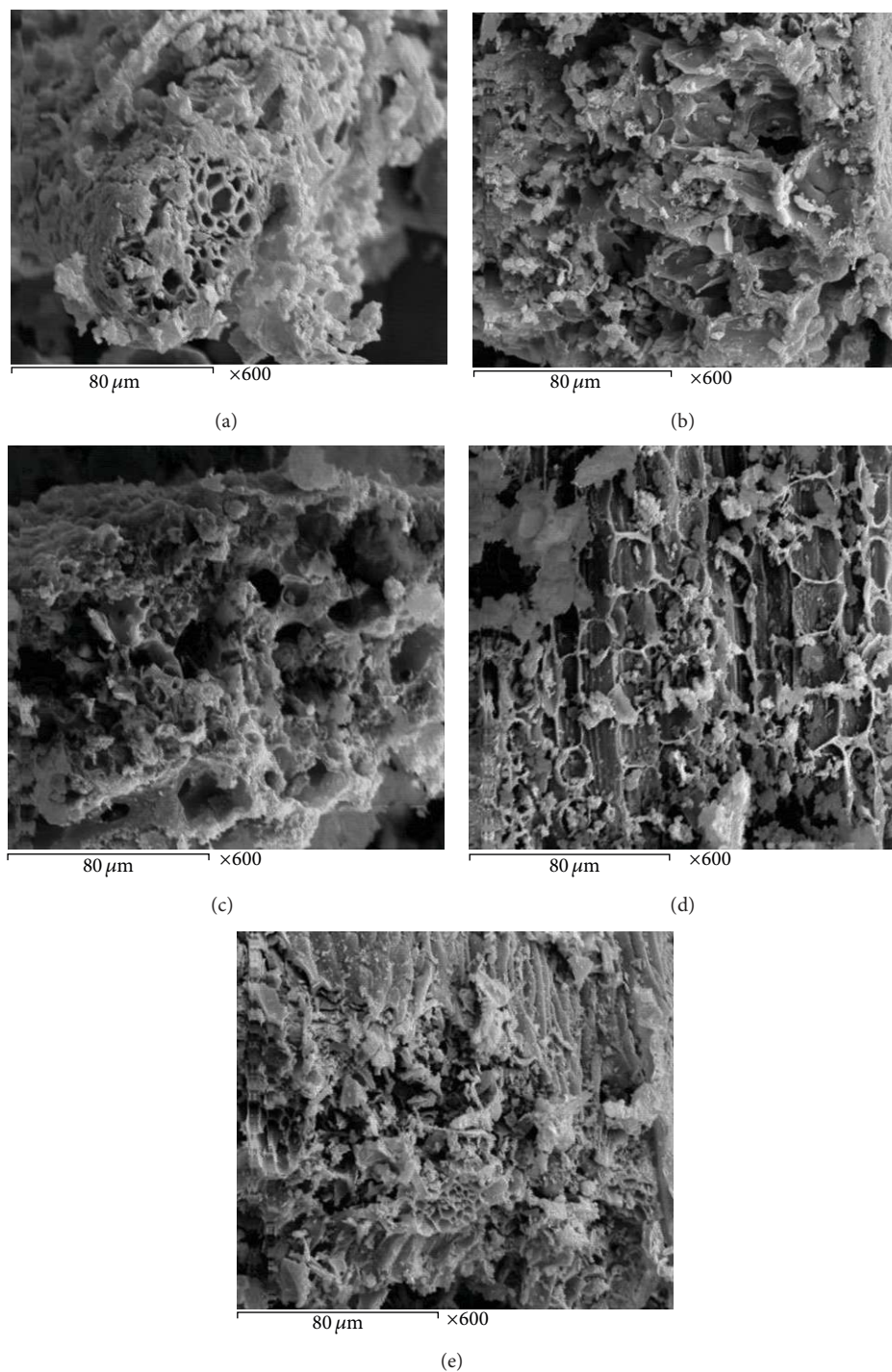


FIGURE 1: SEM micrographs for (a) raw Palm shell, (b) 20% H_3PO_4 , (c) 50% H_3PO_4 , (d) K_2CO_3 , and (e) steam.

than the pH_{pzc} while anions adsorption will be favorable at pH values lower than pH_{pzc} . It has been reported by earlier researchers [22] that the pH_{pzc} of an adsorbent decreases with increase in acidic groups on the surface of the adsorbents. From these results, it can be concluded that acid activation of the Palm tree branches enhanced positive surface charges on the adsorbent surface since the pH_{pzc} for the adsorbents treated with 20% and 50% H_3PO_4 was found to be 4.3 and

3.7, respectively. However, for the steam and K_2CO_3 activated Palm tree branches, the increase in pH_{pzc} relative to the raw sample is due to the modification of the surface after activation [22].

3.5. Adsorption Isotherms. Adsorption isotherms indicate how the adsorption molecules distribute between the liquid

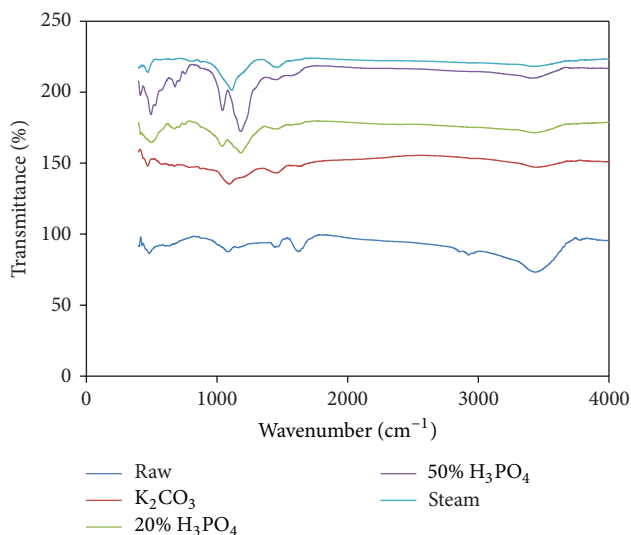


FIGURE 2: FTIR spectra of raw and different treated adsorbents.

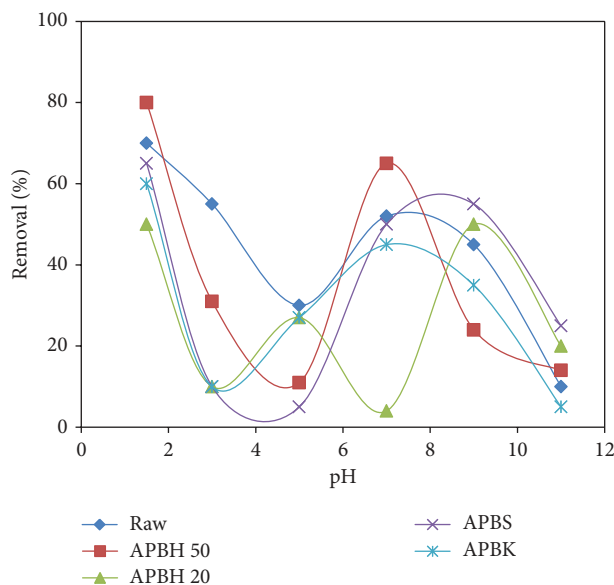


FIGURE 3: Variation of solution pH on percentage removal of Cr(VI) for different adsorbents.

phase and the solid phase when the adsorption process reaches an equilibrium state. Several adsorption isotherms are available and readily adopted to correlate with adsorption equilibrium. In the present study, adsorption of Cr(VI) removal was modeled using the Langmuir, Freundlich, and Flory-Huggins isotherm models. To appreciate which model describes better the sorption of Cr(VI) onto different treated modified adsorbents, the values of the regression correlation coefficients (R^2) were compared.

3.5.1. Langmuir Isotherm. Langmuir adsorption isotherm model [23] is based on an assumption that the adsorption occurs at specific homogeneous sites within the adsorbent and the monolayer adsorption onto a surface containing a

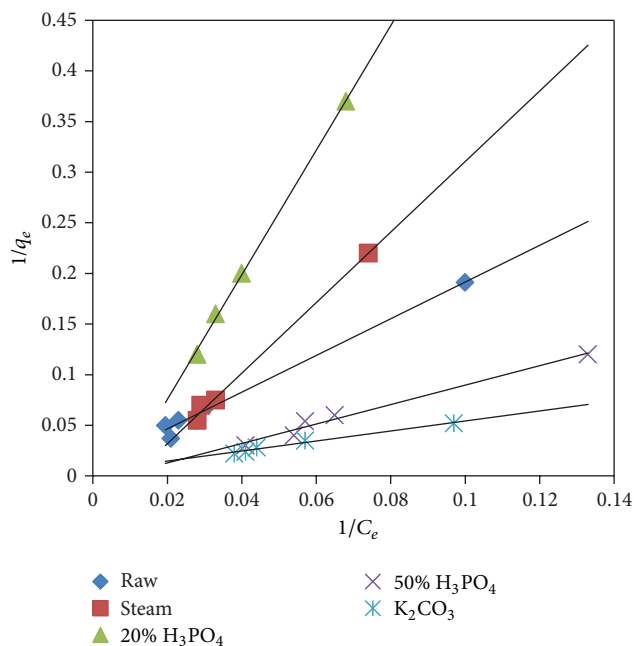


FIGURE 4: Langmuir isotherm plot for adsorption of Cr(VI) onto different treated adsorbents.

finite number of adsorption sites with no transmigration of adsorbate in the plane of surface. The Langmuir isotherm is expressed as

$$\frac{1}{q_e} = \frac{1}{Q_o K_L C_e} + \frac{1}{Q_o}, \quad (3)$$

where C_e is the equilibrium concentration of the adsorbate (mg L^{-1}), q_e is the amount of adsorbate per unit mass of adsorbent (mg g^{-1}), Q_o is the maximum adsorption capacity (mg g^{-1}), and K_L is Langmuir constant related to energy of adsorption capacity (L mg^{-1}).

The linear plot of $1/q_e$ versus $1/C_e$ is shown in Figure 4. The constants Q_o and K_L can be calculated from slope and intercept of the plot and the values are tabulated in Table 2. The essential characteristics of the Langmuir isotherm can be expressed in terms of a dimensionless equilibrium parameter (R_L) which is defined by

$$R_L = \frac{1}{1 + K_L C_o}. \quad (4)$$

The calculated values of R_L are included in Table 2. The value of R_L indicates the type of the isotherm to be either favorable ($0 < R_L < 1$), unfavorable ($R_L > 1$), linear ($R_L = 1$), or irreversible ($R_L = 0$). The value of R_L was found to be less than one in all cases and this confirmed that the Langmuir isotherm model was favorable for adsorption of Cr(VI) onto the activated carbons used in this study. Most of the studies from literature reported that the Langmuir model was more suitable for describing the adsorption isotherm of Cr(VI) onto adsorbents [24, 25]. Differences in Cr(VI) adsorption capacities of the different activated Palm tree branches resulted from the properties of adsorbents

TABLE 2: Equilibrium isotherm constants of Cr(VI) adsorption onto raw and different activated adsorbents.

Model		Adsorbents				
		RPB	APBH 20	APBH 50	APBS	APBK
Langmuir	Q_o	25	37	59	20	50
	K_L	0.023	0.037	0.037	0.031	0.023
	R^2	0.99	0.99	0.98	0.99	0.98
Freundlich	K_F	0.23	2.3	4.5	2.7	6.02
	n	1.03	1.05	1.1	1.75	1.14
	R^2	0.91	0.93	0.92	0.93	0.92
Flory-Huggins	K_{FH}	0.02	0.017	0.027	0.019	0.045
	α	3.4	0.79	1.5	1.2	1.68
	R^2	0.91	0.90	0.90	0.92	0.92
	ΔG°	-32.2	-31.1	-32.7	-33.0	-34.8

such as high specific surface area, porous structure, surface characteristics, and operating conditions of the adsorbent. Typically the larger the surface area of the adsorbent, the higher the adsorption capacity [26]. This is found to be in good agreement with the results given in Table 1.

Table 2 lists the comparison of the different equilibrium isotherm constants of Cr(VI) on various adsorbents adsorbed. Inspection of Table 2 reveals that the highest adsorption capacity was observed for the activated sample with 50% H_3PO_4 . This can be explained on the basis that acid activation increased the porosity of the activated carbon. However, for steam activation, the lowest adsorption capacity could be naturally attributed to the presence of high ash content which contributes negatively to the porosity. Also, steam activation was noticed to destruct the internal porosity of the activated carbon. This result is also confirmed from the SEM results in the previous section of this paper [27].

3.5.2. Freundlich Isotherm. Freundlich isotherm assumes that the uptake of metal ions occurs on a heterogeneous surface by multilayer adsorption and that the amount of adsorbate adsorbed increases infinitely with an increase in concentration [28].

The well-known linear form of Freundlich model is expressed by

$$\log q_e = \log K_F + \frac{1}{n} \log C_e, \quad (5)$$

where K_F ($L\ mg^{-1}$) and $1/n$ are Freundlich constants representing the adsorption capacity and intensity of adsorption, respectively. Isotherms with $n > 1$ are classified as L-type isotherms reflecting a high affinity between adsorbate and adsorbent and are indicative of chemisorption. The values of K_F and n were obtained from the slope and intercept of the plot of $\log q_e$ versus $\log C_e$ and are given in Table 2. From Table 2, the value of n is greater than unity, indicating that Cr(VI) ions were favorably adsorbed on the activated carbons investigated.

3.5.3. Flory-Huggins Isotherm. The Flory-Huggins model was used to determine the degree of surface coverage characteristics of the adsorbate on the adsorbent [29]. The linear form of the Flory-Huggins equation is expressed as

$$\log \left(\frac{\theta}{C_o} \right) = \log K_{FH} + \alpha_{FH} \log (1 - \theta), \quad (6)$$

where $\theta = (1 - C_e/C_o)$ is the degree of surface coverage of the adsorbent by adsorbate and K_{FH} and α_{FH} are the Flory-Huggins constants. These constants can be obtained from the plot of $\log(\theta/C_o)$ versus $\log(1 - \theta)$ (figure not shown). The data is represented in Table 2. Furthermore, the equilibrium constant K_{FH} , obtained from the Flory-Huggins equation, is used to compute the Gibbs free energy for the adsorption process. The Gibbs free energy is related to the equilibrium constant by the following equation:

$$\Delta G^\circ = -RT \ln K_{FH}, \quad (7)$$

where R is the universal gas constant = $8.314\ J\ mol^{-1}$, T is the absolute temperature (K), and K_{FH} is the Flory-Huggins equilibrium constant. The negative values of ΔG° (Table 2) indicate that the adsorption of Cr(VI) onto Palm tree branches is spontaneous in nature and supports an exothermic reaction. From the correlation coefficients (R^2) reported in Table 2, the Langmuir adsorption isotherm yielded best fit as indicated by the highest (R^2) values (>0.98) for the different activated carbon adsorbents studied.

4. Kinetic Studies

Three simplified kinetic models, namely, pseudo-first-order, pseudo-second-order, and intraparticle diffusion models, have been discussed to identify the rate and kinetics of sorption of Cr(VI) removal onto different activated Palm tree branches [30].

4.1. Pseudo-First-Order Kinetic Model. The pseudo-first-order reaction equation (Lagergren's rate equation) is one

TABLE 3: Kinetic parameters for the adsorption of Cr(VI) onto different activated Palm tree branches.

Kinetic model		Adsorbents				
		RPB	APBH 20	APBH 50	APBS	APBK
Pseudo-first-order	K_1 (min^{-1})	0.013	0.015	0.062	0.013	0.017
	q_e (mg g^{-1})	79.0	36.3	120	100	66.1
	R^2	0.91	0.90	0.92	0.91	0.92
Pseudo-second-order	K_2 ($\text{g mg}^{-1} \text{min}^{-1}$)	9.1×10^{-5}	2.9×10^{-3}	2.2×10^{-4}	1.3×10^{-4}	1.4×10^{-3}
	q_e (mg g^{-1})	187	91.8	157	113	83.0
	R^2	0.99	0.98	0.99	0.99	0.98
Intraparticle diffusion	K_p ($\text{mg g}^{-1} \text{min}^{-1/2}$)	8.40	2.30	13.8	3.60	8.20
	R^2	0.90	0.91	0.91	0.90	0.92

of the most widely used rate equations to describe the adsorption of an adsorbate from the liquid phase [31]. The first-order rate equation is represented as

$$\log(q_e - q_t) = \log q_e - \frac{K_1}{2.303} t, \quad (8)$$

where q_e and q_t are the amount of adsorbed Cr(VI) on the adsorbent at equilibrium and at time t , respectively (mg g^{-1}), and K_1 is the first-order adsorption rate constant (min^{-1}). The values of q_e and K_1 for the pseudo-first-order kinetic model were determined from the intercepts and slopes of the plots of $\log(q_e - q_t)$ versus t (figure not shown). The calculated results of the first-order rate equation are given in Table 3.

4.2. Pseudo-Second-Order Kinetic Model. This model assumes that two reactions are occurring; the first one is fast and reaches equilibrium quickly and the second is a slower reaction that can continue for a long period of time [32].

The kinetics of adsorption can be represented by the pseudo-second-order equation in the following form [33]:

$$\frac{t}{q_t} = \frac{1}{K_2 q_e^2} + \frac{1}{q_e} t, \quad (9)$$

where K_2 is the rate constant of the pseudo-second-order adsorption ($\text{g mg}^{-1} \text{min}^{-1}$). The plot of t/q_t versus t is a straight line as shown in Figure 5. The K_2 and q_e values determined from the slope and intercept of the plot are given in Table 3 along with the correlation coefficients. As can be seen from Table 3, the correlation coefficients (R^2) obtained from pseudo-second-order model were found to be higher than 0.98 for all activated Palm tree branches which were larger than those of the pseudo-first-order model. The results revealed that the pseudo-second-order model was the best one in describing the kinetics of Cr(VI) adsorbed onto the different modified samples.

4.3. Intraparticle Diffusion. Kinetic data was further analyzed using the intraparticle diffusion model based on the theory proposed by Weber and Morris [34].

The adsorbate transport from the solution phase to the surface of the adsorbent particles occurs in several steps. The overall adsorption process may be controlled either by one or more steps, for example, film diffusion, pore diffusion,

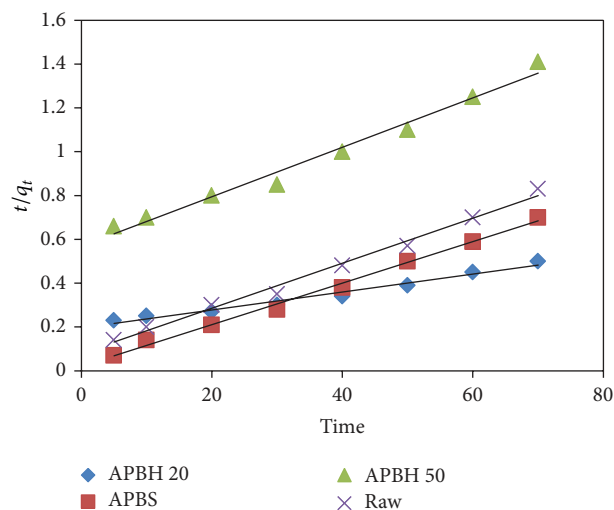


FIGURE 5: Pseudo-second-order kinetics for adsorption of Cr(VI) onto different treated adsorbents.

surface diffusion, and adsorption on the pore surface, or a combination of more than one step. The rate parameters for intraparticle diffusion (K_{id}) for Cr(VI) removal were determined by using the following equation:

$$q_t = K_{id} t^{1/2} + C, \quad (10)$$

where K_{id} is the rate constant of intraparticle diffusion parameter ($\text{mg g}^{-1} \text{min}^{-1/2}$) and C is the intercept. The values of K_{id} and C can be determined from the slope and intercept of the plot q_t versus $t^{1/2}$ and are listed in Table 3 (Figure 6). Values of C give an idea about the thickness of boundary layer; that is, the larger the intercept, the greater the contribution of the surface sorption in the rate controlling step [35]. Based on this plot (Figure 6), it was concluded that the sorption process of Cr(VI) is comprised of two phases, suggesting that intraparticle diffusion mechanism is not the rate limiting step for the whole reaction. The initial portion of the plot indicated an external mass transfer whereas the second linear portion is due to intraparticle or pore diffusion. The two phases in the intraparticle diffusion plot suggest that the adsorption of Cr(VI) ions proceed by surface sorption and intraparticle diffusion.

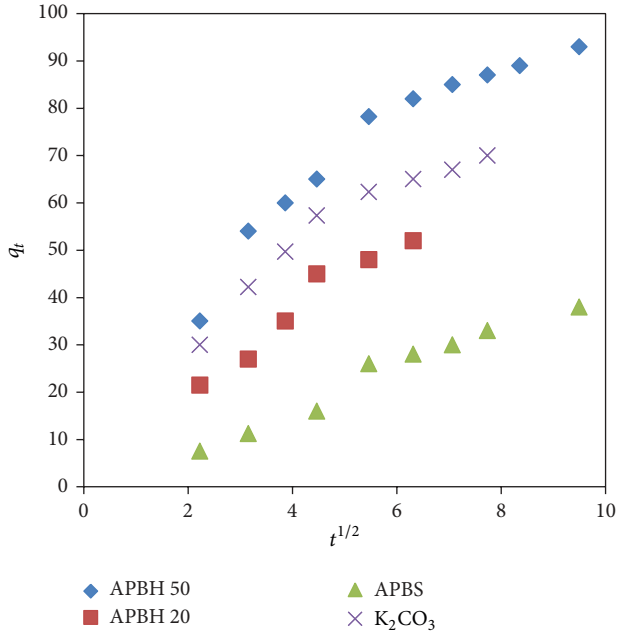


FIGURE 6: Intraparticle diffusion plots for Cr(VI) adsorption onto different adsorbents studied.

5. Column Studies

Breakthrough curves are very important characteristics for determining the operation and the dynamic response of an adsorption column. The loading behavior of Cr(VI) to be removed from the solution in a fixed bed is usually expressed in terms of C_t/C_o where (C_t = effluent of Cr(VI) ion concentration and C_o = influent of Cr(VI) ion concentration in mg L^{-1}). C_t/C_o is then plotted against bed volume in order to obtain the breakthrough curve. The maximum column capacity, q_{total} (mg), for a given feed concentration and flow rate is equal to the area under the plot of the adsorbed Cr(VI) concentration and is calculated as follows [11]:

$$q_{\text{total}} = \frac{QA}{1000} = \frac{Q}{1000} \int_{t=0}^{t=t_{\text{total}}} C_{\text{ad}} dt, \quad (11)$$

where $C_{\text{ad}} = C_o - C_t$, t_{total} is the total flow time (min), Q is the volumetric flow rate (mL/min), and A is the area under the breakthrough curve. The equilibrium uptake (q_{eq}) is calculated as follows:

$$q_{\text{eq}} = \frac{q_{\text{total}}}{m}, \quad (12)$$

where m is the total dry weight of modified palm tree branches in column (g). The total amount of Cr(VI) sent to the column (M_{total}) is calculated from the equation below:

$$m_{\text{total}} = \frac{C_o Q t_{\text{total}}}{1000}. \quad (13)$$

The total removal is calculated from the following equation:

$$\text{Total removal\%} = \frac{q_{\text{total}}}{m_{\text{total}}} \times 100. \quad (14)$$

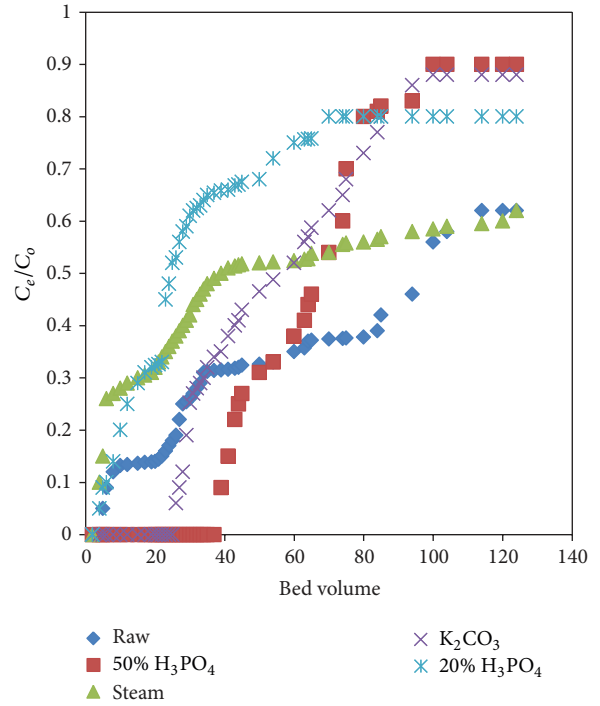


FIGURE 7: Breakthrough curves for Cr(VI) adsorption onto different adsorbents.

TABLE 4: Column parameters for the adsorption of Cr(VI) onto raw and different activated carbon samples.

Sample	t_{total} (min)	m_{total} (mg)	q_{total} (mg)	Total metal removal (%)
RPB	250	50	7	13.6
APBH 20	300	60	10	18.6
APBH 50	420	85	39	55.1
APBS	355	71	28	47.2
APBK	175	35	7	11.9

Figure 7 shows the dynamic adsorption of Cr(VI) in columns packed with raw and different activated carbon samples. It can be seen from the curve that the breakthrough of the Cr(VI) was 60 bed volumes (BV) for the sample activated with 50% H_3PO_4 , while that activated with K_2CO_3 reached 50 BV. However, for the raw and activated samples with 20% H_3PO_4 and steam, the bed volumes were found to be 3 BV, 2 BV, and 1 BV, respectively. It appears that the Palm branches activated with 50% H_3PO_4 are more selective for Cr(VI) adsorption than the other activated Palm tree branches [11] as shown in Table 4.

6. Desorption Studies

Desorption is a phenomenon or process where some of the adsorbed substance is released. The adsorption of solute on any sorbent can be carried out either by physical bonding, ion exchange, or combination of both. The desorption can be effected by stronger desorbate like acid or alkali solutions.

The desorption efficiency results revealed 93%, 42%, 23%, and 20% for samples activated with 50% H_3PO_4 , K_2CO_3 , raw, and 20% H_3PO_4 , respectively, with 1 M HCl while the sample activated with steam showed 8%.

The desorption of Cr(VI) on the different treated activated carbons can be explained on the basis of forces (physical and chemical) involved in the adsorption process. Physically bonded molecules get desorbed easily by 1M HCl while chemically bonded molecules were not desorbed completely. This may be due to the formation of a strong complexation compound on the surface of the activated carbon [16].

7. Conclusion

The present study focused on the adsorption of Cr(VI) from aqueous solution using activated Palm tree branches as effective adsorbents. Adsorption of Cr(VI) was found to be effective in the lower pH range, being attributed to the presence of excess positive charge on the surface of palm tree branches activated with 50% H_3PO_4 . Adsorption of Cr(VI) could be adequately described by Langmuir ($R^2 > 0.98$) isotherm. Kinetic study showed that the pseudo-second-order is appropriate to describe the experimental and controlled by both film and pore diffusions that might be involved in the sorption process. Desorption of Cr(VI) was promising for the Palm tree branches treated with 50% H_3PO_4 .

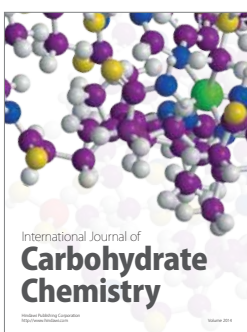
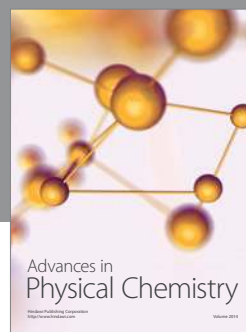
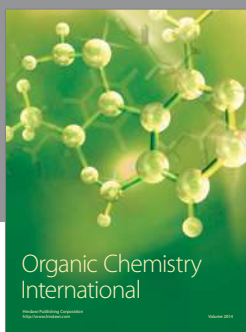
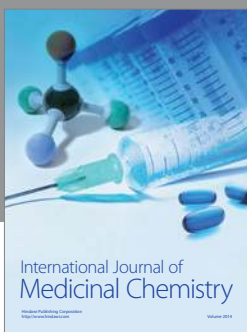
Conflict of Interests

The authors declare that there is no conflict of interests regarding the publication of this paper.

References

- [1] H. K. An, B. Y. Park, and D. S. Kim, "Crab shell for the removal of heavy metals from aqueous solution," *Water Research*, vol. 35, no. 15, pp. 3551–3556, 2001.
- [2] N. Febriana, S. O. Lesmana, F. Q. Soetaredjo, J. Sunarso, and S. Ismadji, "Neem leaf utilization for copper ions removal from aqueous solution," *Journal of the Taiwan Institute of Chemical Engineers*, vol. 41, no. 1, pp. 111–114, 2010.
- [3] K. Mohanty, M. Jha, B. C. Meikap, and M. N. Biswas, "Removal of chromium (VI) from dilute aqueous solutions by activated carbon developed from *Terminalia arjuna* nuts activated with zinc chloride," *Chemical Engineering Science*, vol. 60, no. 11, pp. 3049–3059, 2005.
- [4] US EPA, *IRIS, Integrated Risk Information System*, US Environmental Protection Agency, Washington, DC, USA, 1997.
- [5] C. Raji and T. S. Anirudhan, "Kinetics of Pb(II) adsorption by polyacrylamide grafted sawdust," *Indian Journal of Chemical Technology*, vol. 4, no. 3, pp. 157–162, 1997.
- [6] S. S. Ahluwalia and D. Goyal, "Microbial and plant derived biomass for removal of heavy metals from wastewater," *Biore-source Technology*, vol. 98, no. 12, pp. 2243–2257, 2007.
- [7] A. Baran, E. Bicak, S. Hamarat, and O. S. Baysal, "Comparative studies on the adsorption of Cr(VI) ions on to various sorbents," *Biore-source Technology*, vol. 98, no. 3, pp. 661–665, 2006.
- [8] S. Gupta and B. V. Babu, "Adsorption of Chromium by a low cost adsorbent prepared from tamarind seeds," in *Proceedings of the International Symposium and 59th Annual Session of IChE in Association with International Partners (CHEMCON '06)*, pp. 27–30, GNFC Complex, Bharuch, India, December 2006.
- [9] R. C. Bansal and M. Goyal, *Activated Carbon Adsorption*, Taylor & Francis, Boca Raton, Fla, USA, 2005.
- [10] H. Marsh and F. R. Reinoso, *Activated Carbon*, Elsevier, San Diego, Calif, USA, 2006.
- [11] H.-D. Choi, W.-S. Jung, J.-M. Cho, B.-G. Ryu, J.-S. Yang, and K. Baek, "Adsorption of Cr(VI) onto cationic surfactant-modified activated carbon," *Journal of Hazardous Materials*, vol. 166, no. 2–3, pp. 642–646, 2009.
- [12] K. Selvi, S. Pattabhi, and K. Kadirvelu, "Removal of Cr(VI) from aqueous solution by adsorption onto activated carbon," *Biore-source Technology*, vol. 80, no. 1, pp. 87–89, 2001.
- [13] H.-D. Choi, M.-C. Shin, D.-H. Kim, C.-S. Jeon, and K. Baek, "Removal characteristics of reactive black 5 using surfactant-modified activated carbon," *Desalination*, vol. 223, no. 1–3, pp. 290–298, 2008.
- [14] Y. Sudaryanto, S. B. Hartono, W. Irawaty, H. Hindarso, and S. Ismadji, "High surface area activated carbon prepared from cassava peel by chemical activation," *Biore-source Technology*, vol. 97, no. 5, pp. 734–739, 2006.
- [15] L. S. Clesceri, A. E. Greenberg, and A. D. Eaton, "Standard methods for the examination of Water & Waste Water," in *Proceedings of the 20th American Public Health Association*, pp. 3-65–3-68, Washington, DC, USA, 1998.
- [16] M. Gholipour and H. Hashemipour, "Hexavalent chromium removal from aqueous solution via adsorption on granular activated carbon: adsorption, desorption, modeling and simulation studies," *Journal of Engineering and Applied Sciences*, vol. 6, no. 9, pp. 10–18, 2011.
- [17] A. R. Yacob, Z. A. Majid, R. S. D. Darsil, and V. A. Inderan, "Comparison of various sources of high surface area carbon prepared by different types of activation," *The Malaysian Journal of Analytical Sciences*, vol. 12, no. 1, pp. 264–271, 2008.
- [18] M. Imamoglu and O. Tekir, "Removal of copper (II) and lead (II) ions from aqueous solutions by adsorption on activated carbon from a new precursor hazelnut husks," *Desalination*, vol. 228, no. 1–3, pp. 108–113, 2008.
- [19] B. Bayat, "Comparative study of adsorption properties of Turkish fly ashes: II. The case of chromium (VI) and cadmium (II)," *Journal of Hazardous Materials*, vol. 95, no. 3, pp. 275–290, 2002.
- [20] C. Namasivayam and K. Ranganathan, "Waste Fe(III)/Cr(III) hydroxide as adsorbent for the removal of Cr(VI) from aqueous solution and chromium plating industry wastewater," *Environmental Pollution*, vol. 82, no. 3, pp. 255–261, 1993.
- [21] S. M. Nomanbhay and K. Palanisamy, "Removal of heavy metal from industrial wastewater using chitosan coated oil palm shell charcoal," *Electronic Journal of Biotechnology*, vol. 8, no. 1, pp. 43–53, 2005.
- [22] T. S. Anirudhan and K. A. Krishnan, "Removal of cadmium(II) from aqueous solutions by steam-activated sulphurised carbon prepared from sugar-cane bagasse pith: kinetics and equilibrium studies," *Water SA*, vol. 29, no. 2, pp. 147–156, 2003.
- [23] I. Langmuir, "The adsorption of gases on plane surfaces of glass, mica and platinum," *The Journal of the American Chemical Society*, vol. 40, no. 9, pp. 1361–1403, 1918.
- [24] K. Baek, B.-K. Kim, H.-J. Cho, and J.-W. Yang, "Removal characteristics of anionic metals by micellar-enhanced ultrafiltration," *Journal of Hazardous Materials*, vol. 99, no. 3, pp. 303–311, 2003.

- [25] K. Baek and J.-W. Yang, "Cross-flow micellar-enhanced ultrafiltration for removal of nitrate and chromate: competitive binding," *Journal of Hazardous Materials*, vol. 108, no. 1-2, pp. 119–123, 2004.
- [26] I. A. W. Tan, A. L. Ahmad, and B. H. Hameed, "Enhancement of basic dye adsorption uptake from aqueous solutions using chemically modified oil palm shell activated carbon," *Colloids and Surfaces A: Physicochemical and Engineering Aspects*, vol. 318, no. 1-3, pp. 88–96, 2008.
- [27] H. Teng, J.-A. Ho, Y.-F. Hsu, and C.-T. Hsieh, "Preparation of activated carbons from bituminous coals with CO₂ activation. 1. Effects of oxygen content in raw coals," *Industrial and Engineering Chemistry Research*, vol. 35, no. 11, pp. 4043–4049, 1996.
- [28] H. M. F. Freundlich, "Over the adsorption in the solution," *The Journal of Physical Chemistry*, vol. 57, pp. 358–470, 1906.
- [29] A. Ergene, K. Ada, S. Tan, and H. Katircioglu, "Removal of Remazol Brilliant Blue R dye from aqueous solutions by adsorption onto immobilized *Scenedesmus quadricauda*: equilibrium and kinetic modeling studies," *Desalination*, vol. 249, no. 3, pp. 1308–1314, 2009.
- [30] N. K. Hamadi, X. D. Chen, M. M. Farid, and M. G. Q. Lu, "Adsorption kinetics for the removal of chromium(VI) from aqueous solution by adsorbents derived from used tyres and sawdust," *Chemical Engineering Journal*, vol. 84, no. 2, pp. 95–105, 2001.
- [31] S. Lagergren, "Zur theorie der sogenannten adsorption gelöster stoffe," *Kungliga Svenska Vetenskapsakademiens Handlingar*, vol. 24, no. 4, pp. 1–39, 1898.
- [32] C. K. Ko, C. W. Cheung, K. K. Choy, J. F. Porter, and G. McKay, "Sorption equilibria of metal ions on bone char," *Chemosphere*, vol. 54, no. 3, pp. 273–281, 2004.
- [33] Y. S. Ho and G. McKay, "Pseudo-second order model for sorption processes," *Process Biochemistry*, vol. 34, no. 5, pp. 451–465, 1999.
- [34] W. J. Weber and J. C. Morris, "Intraparticle diffusion during the sorption of surfactants onto activated carbon," *Journal of Sanitary Engineering Division American Society for Civil Engineers*, vol. 89, pp. 53–61, 1963.
- [35] S. Arivoli, M. Hema, M. Karuppaiah, and S. Saravanan, "Adsorption of chromium ion by acid activated low cost carbon-kinetic, mechanistic, thermodynamic and equilibrium studies," *E-Journal of Chemistry*, vol. 5, no. 4, pp. 820–831, 2008.



Hindawi

Submit your manuscripts at
<http://www.hindawi.com>

